CCAR2 Is Required for Proliferation and Tumor Maintenance in Human Squamous Cell Carcinoma

Sarah A. Best[1,2], Amy N. Nwaobasi[1], Chrysalyne D. Schmults[1,2] and Matthew R. Ramsey[1,2]

CCAR2 is a widely expressed protein involved in the regulation of a variety of transcriptional complexes. High expression of CCAR2 correlates with poor outcomes in many human tumor types such as squamous cell carcinoma (SCC). Paradoxically, loss of *Ccar2* in the mouse results in an increased tumor burden, suggesting that CCAR2 may in fact function as a tumor suppressor. This tumor suppressor function is dependent on p53, a protein that is inactivated in the vast majority of SCC tumors, leaving the role of CCAR2 in *p53*-null tumors unclear. We sought to identify p53-independent CCAR2 functions in SCC and to examine its role in tumorigenesis. We found that CCAR2 is highly overexpressed in *p53*-deficient SCC cell lines compared with normal primary keratinocytes due to increased protein stability. We identify a role for CCAR2 in promoting the stability of the transcription factors RFX1 and CREB1, which are both required for proliferation. Finally, we show that CCAR2 is required for proliferation in vitro and in established SCC tumors in vivo. Our data suggest an important role for CCAR2 in maintaining cell cycle progression and promoting SCC tumorigenesis.

Journal of Investigative Dermatology (2017) **137,** 506–512; doi:10.1016/j.jid.2016.09.027

INTRODUCTION

Non-melanoma skin cancer is the most common form of cancer, and although most patients have positive outcomes, a subset of patients succumb to metastatic disease (Karia et al., 2013). Clinical studies across a variety of tumor types, including SCC, have suggested that high levels of CCAR2 (also known as DBC1) may be an indicator of poor outcomes (Chen et al., 2014; Kim et al., 2013; Kim et al., 2012; Yu et al., 2013) and could potentially have pro-tumorigenic functions. However, studies in *Ccar2*$^{-/-}$ mice suggest that Ccar2 may function as a tumor suppressor, although SCC did not develop in these mice (Qin et al., 2015).

CCAR2 has been shown to bind and inhibit the nicotinamide adenine dinucleotide-dependent deacetylase activity of SIRT1 (Kim et al., 2008; Zhao et al., 2008). The CCAR2-SIRT1 complex is dynamically regulated by nutrient levels, as fasting results in dissociation to release highly active SIRT1, whereas high nutrient levels promote the SIRT1-CCAR2 association, blocking SIRT1 deacetylase activity (Escande et al., 2010; Nin et al., 2014). In addition, the CCAR2-SIRT1 interaction can be inhibited through acetylation of CCAR2 by hMOF (Zheng et al., 2013) or enhanced through phosphorylation of CCAR2 by ATM/ATR kinases in response to DNA damage (Yuan et al., 2012; Zannini et al., 2012). Inhibition of SIRT1 activity by CCAR2 after DNA damage results in acetylation and activation of p53, which can then activate downstream targets (Kim et al., 2008; Luo et al., 2001; Vaziri et al., 2001; Zhao et al., 2008). In addition, CCAR2 can regulate the function of a variety of transcription factors through inhibition of SIRT1-dependent deacetylation (Chini CC et al., 2013; Huan et al., 2015; Kim et al., 2015; Koyama et al., 2010; Park et al., 2013; Sakurabashi et al., 2015; Tanikawa et al., 2013; Yu et al., 2016).

In this study, we sought to clarify the role of CCAR2 in squamous cell carcinoma (SCC). We show that SCC cells stabilize CCAR2 protein, leading to significant overexpression, and that CCAR2 is essential for continued proliferation of SCC tumors, independent of p53 function. We have identified key transcription factors, CREB and RFX1, which bind to and are stabilized by CCAR2. Finally, we show that both CREB and RFX1 are required for the maintenance of proliferation in SCC.

RESULTS

CCAR2 protein expression is elevated in SCC

To understand the role of CCAR2 in SCC, we examined CCAR2 expression in the normal epidermis and cutaneous SCC (Figure 1a). In normal skin, CCAR2 was expressed in both the interfollicular epidermis and the hair follicle. Similar to esophageal SCC (Kim et al., 2012), CCAR2 was also expressed in cutaneous SCC (Figure 1a). Examination of cultured primary human and murine keratinocytes and SCC cell lines from the epidermis (SCC-13), oral cavity (SCC-25, HO1N1), and larynx (JHU-029) by Western blot identified a large increase in CCAR2 protein in SCC cells compared with keratinocytes (Figure 1b, and see Supplementary Figure S1a online). One major function of CCAR2 is to inhibit the deacetylase activity of SIRT1 through direct interaction (Kim et al., 2008; Zhao et al., 2008), and high SIRT1 expression correlates with poor prognosis in SCC (Chen et al., 2014).

[1]Brigham and Women's Hospital, Boston, Massachusetts, USA; and [2]Harvard Medical School, Department of Dermatology, Boston, Massachusetts, USA

Correspondence: Matthew R. Ramsey, Brigham and Women's Hospital, 77 Avenue Louis Pasteur, HIM 668, Boston, Massachusetts 02115, USA. E-mail: mramsey@bwh.harvard.edu

Abbreviations: shRNA, short hairpin RNA; SCC, squamous cell carcinoma

Received 11 March 2016; revised 21 September 2016; accepted 26 September 2016; accepted manuscript published online 7 October 2016; corrected proof published online 14 November 2016

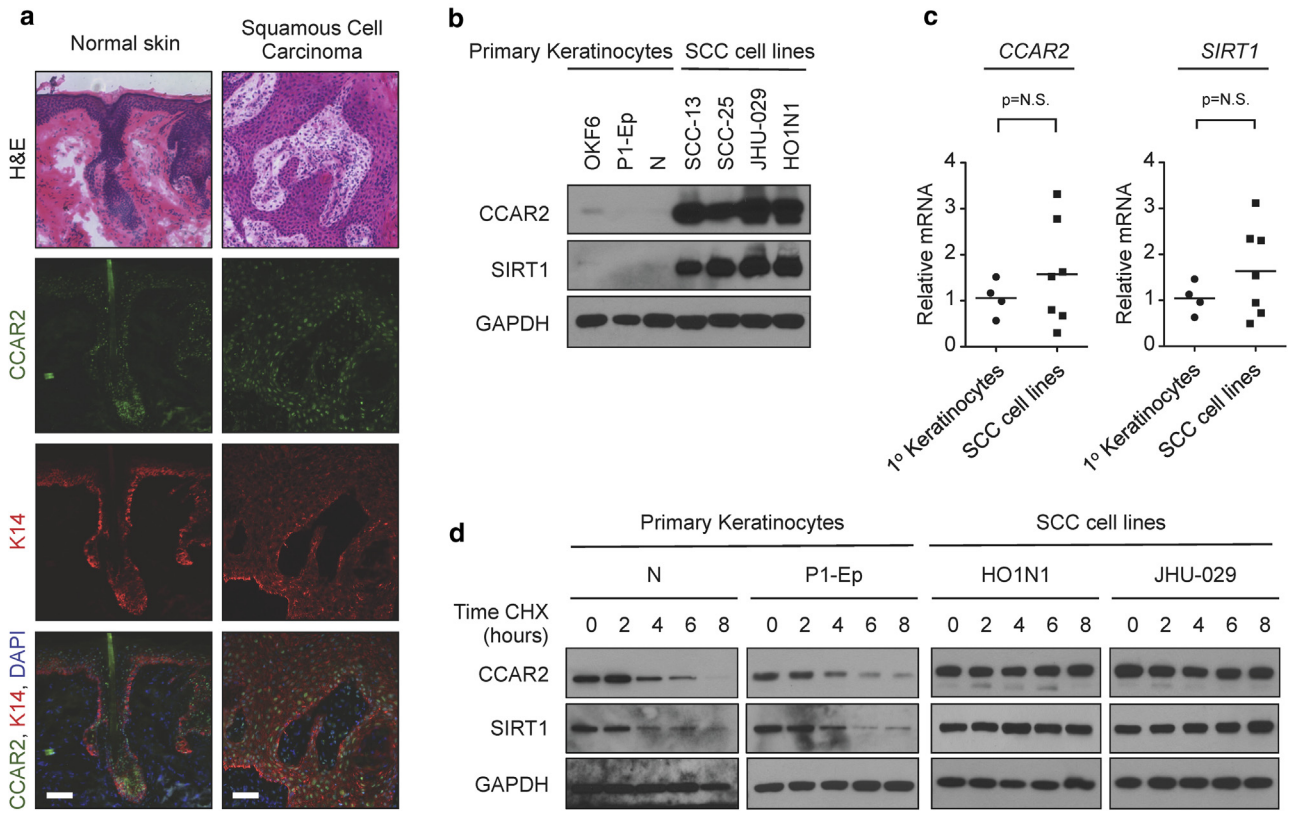

Figure 1. CCAR2 and SIRT1 proteins are stabilized in squamous cell carcinoma. (**a**) Histologic (H&E) and immunofluorescence analysis of CCAR2 (green) and keratin 14 (K14, red) protein expression in normal human skin and SCC frozen sections. DAPI (blue) stains the nucleus. Scale bar = 50 μm. (**b**) Western blot analysis of CCAR2 and SIRT1 protein in primary keratinocytes (OKF6, P1-Ep, and N) and SCC (SCC-13, SCC-25, JHU-029, and HO1N1) cell lines. GAPDH provides the loading control. (**c**) Quantitative real-time PCR of *CCAR2* (left) and *SIRT1* (right) mRNA expression in keratinocytes and SCC cell lines. $P > 0.05$, not significant. (**d**) Western blot of CCAR2 and SIRT1 protein expression in primary keratinocytes (N, P1-Ep) and SCC (HO1N1 and JHU-029) cell lines treated with cyclohexamide (100 μg/ml) for 0, 2, 4, 6, or 8 hours. GAPDH provides the loading control. CHX, cyclohexamide; H&E, hematoxylin and eosin; K14, keratin 14; N.S., not significant; SCC, squamous cell carcinoma.

Similar to CCAR2, we observed an increase in SIRT1 protein in SCC cells compared with normal keratinocytes (Figure 1b, and see Supplementary Figure S1a). Despite the large increases in protein, there was no significant difference in either *CCAR2* or *SIRT1* mRNA levels between primary keratinocytes and SCC cell lines (Figure 1c, and see Supplementary Figure S1b). We treated primary keratinocytes and SCC cells with cycloheximide, an inhibitor of protein translation, and examined CCAR2 and SIRT1 protein by Western blot. In primary keratinocytes, the half-life of both CCAR2 and SIRT1 was between 2 and 4 hours, whereas in SCC cells no detectable decrease in CCAR2 or SIRT1 protein was observed within the 8-hour experiment (Figure 1d, and see Supplementary Figure S1c). These data show that CCAR2 and SIRT1 proteins are more abundant in SCC cells compared with normal keratinocytes due to a significant increase in protein stability.

CCAR2 is required for SCC cell proliferation

To assess the physiological effects of CCAR2 loss, we infected SCC cells with short hairpin RNA (shRNA) targeting *CCAR2* and examined the cell cycle by flow cytometry. After reduction in *CCAR2* levels (see Supplementary Figure S2a online), all cell lines examined (JHU-029, SCC-15, and SCC-25) exhibited a significant increase in the percentage of G2 cells, with a coincident reduction in G1- and S-phase cells (Figure 2a). Consistent with these results, we observed a significant reduction in the colony-forming ability of SCC cells after reduction of CCAR2 levels (Figure 2b, and see Supplementary Figure S2b). Importantly, these cells all have functional inactivation of *p53* caused by frameshift or point mutation (see Supplementary Table S1 online). We then investigated the in vivo requirement for CCAR2 in tumor maintenance. We stably expressed a doxycycline-inducible shRNA directed against *CCAR2* (shCCAR2) or control in tumorigenic JHU-029 cells. Addition of doxycycline results in greater than 50% reduction of CCAR2 protein and mRNA by 48 hours in shCCAR2 cells but not control cells (see Supplementary Figure S2c and d). Cells were injected subcutaneously into *Nude* mice and then treated with doxycycline-containing water after 4 days. Although doxycycline alone had a modest inhibitory effect on tumor growth at early time points, there was a significant reduction in tumor growth in shCCAR2 tumors treated with doxycycline compared with control and shCCAR2 tumors treated with vehicle (Figure 2c). Only the shCCAR2 tumors treated with doxycycline showed reduced CCAR2 protein expression (Figure 2d). Tumors showed no change in cleaved caspase-3 staining, suggesting that CCAR2 does

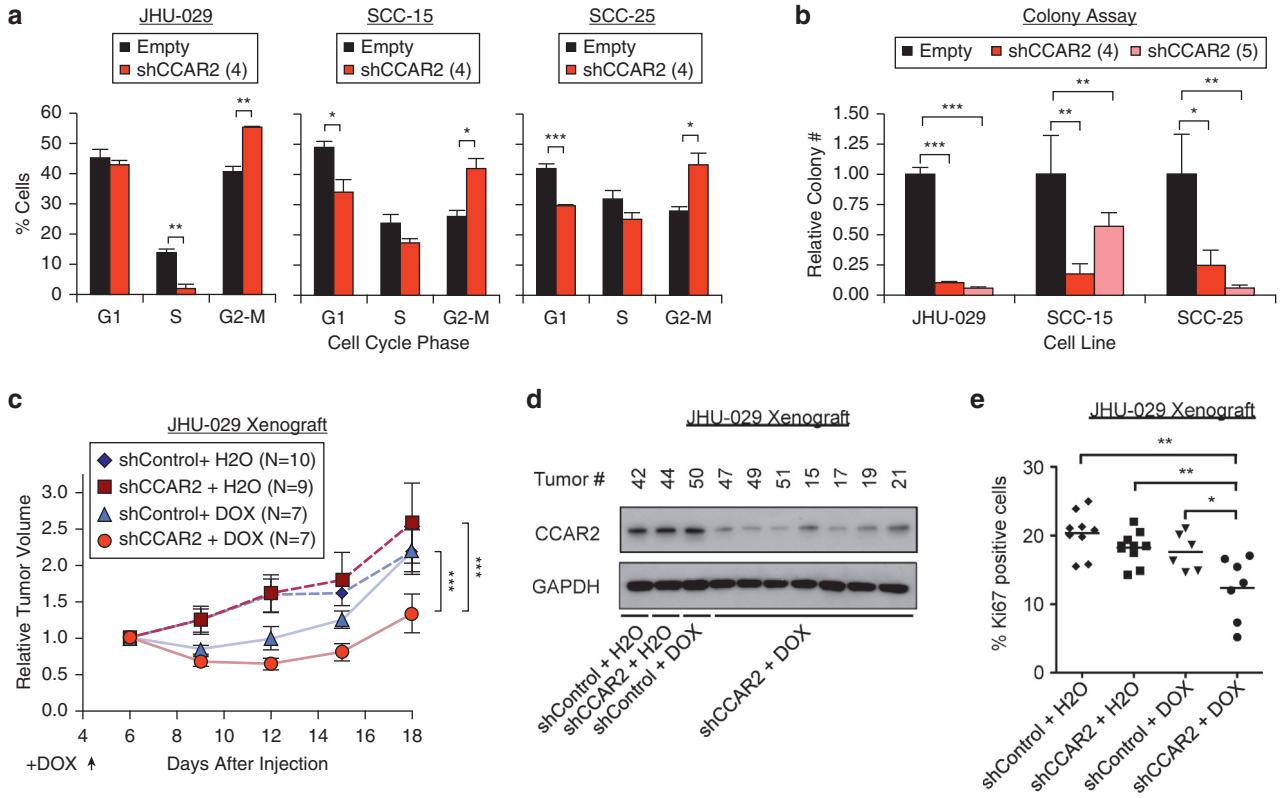

Figure 2. CCAR2 is essential for proliferation and tumor maintenance. (**a**) Flow cytometry analysis of the cell cycle (G1, S, or G2/M) in control (Empty) or *CCAR2*-knockdown (shCCAR2) SCC cell lines. N = 3 replicates. Error bars indicate ± standard deviation. Representative from two independent repeats. (**b**) Colony assay in control or *CCAR2* knockdown SCC cell lines. Colony number is relative to the control of each cell line. Error bars indicate ± standard deviation. N = 4 replicates per cell line. (**c**) Growth of xenograft tumors derived from JHU-029 cells with doxycycline-inducible shRNA, injected subcutaneously in nude mice. Doxycycline was added to drinking water on day 4. Tumor volume is normalized to average day 6 tumor volume for each group. Error bars ± standard error of the mean. (**d**) Western blot analysis of CCAR2 protein in JHU-029 xenograft tumors with indicated treatment as in **c**. (**e**) Analysis of proliferative index of tumors from **c** at day 18 as assessed by Ki67 staining. $*P < 0.05$, $**P < 0.01$, $***P < 0.001$ for all experiments. DOX, doxycycline; SCC, squamous cell carcinoma.

not regulate apoptosis in vivo (see Supplementary Figure S2e). However, there was a significant reduction in Ki67 staining, a marker of proliferation, in shCCAR2 tumors treated with doxycycline compared with all other groups (Figure 2e). These data point to an essential p53-independent role for CCAR2 in promoting SCC cell proliferation and tumor maintenance.

Identification of transcriptional programs regulated by CCAR2

Given the clear requirement for CCAR2 in proliferation, we hypothesized that CCAR2 could regulate one or more transcription factors controlling important cell cycle genes. SCC-13, SCC-15, and HO1N1 cells were infected with shRNA empty vector (Empty) or shRNA directed against *CCAR2* (shCCAR2), cells were harvested after 48 hours, RNA was prepared, and global gene expression profiling was performed using Human HT-12 BeadChip (Illumina Inc, San Diego, CA) arrays. A total of 164 transcripts had a greater than $0.5\log_2$ fold change and a *P*-value of less than 0.05 after *CCAR2* knockdown, with 128 transcripts decreasing expression and 36 transcripts increasing expression (see Supplementary Table S2 online). Pathway and gene ontogeny analysis of this dataset was then performed using the Database for Annotation, Visualization, and Integrated Discovery (DAVID) tool (Dennis et al., 2003). The large majority of gene ontogeny terms and pathways centered on the cell cycle, in particular genes involved in DNA synthesis and mitosis (see Supplementary Tables S3 and S4 online). Examination of transcripts identified by DAVID analysis showed that most of these genes promoted cell cycle progression, and expression decreased after loss of CCAR2 (Figure 3a). Using quantitative real-time PCR, we validated decreases in mitotic genes (*AURKB, INCENP, CDCA7, CDCA5, ASPM,* and *NCAPD2)* 48 hours after shRNA knockdown of *CCAR2* in SCC-13 and HO1N1 cells (Figure 3b), confirming the microarray results. These data identify a subset of cell cycle genes controlled by CCAR2, further supporting a key role in promoting proliferation.

CCAR2 regulates stability of RFX1 and CREB to promote proliferation

CCAR2 has been found to regulate a variety of transcription factors in a context-specific manner. Using the DAVID tool, we generated a list of transcription factors with canonical binding sites that are significantly enriched in our microarray gene set (see Supplementary Table S5 online). When CCAR2 expression was depleted in SCC cell lines using shRNA, the proteins (but not mRNA) of a subset of transcription factors, notably RFX1 and CREB, were reduced (Figure 4a, and see Supplementary Figure S3 online). Both

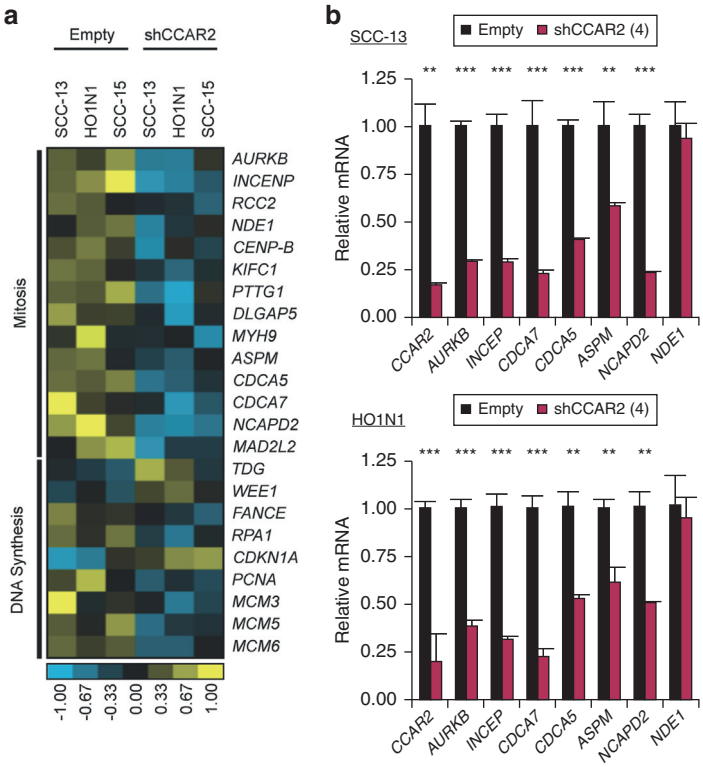

Figure 3. CCAR2 regulates genes involved in cell division. (**a**) Heat map depicting gene expression changes from microarray in *CCAR2* knockdown (shCCAR2) compared with control cells (Empty) in SCC cell lines (SCC-13, HO1N1, SCC-15). (**b**) Quantitative real-time PCR validation of genes identified by the microarray in SCC-13 (top panel) and HO1N1 cells (bottom panel) with either control (Empty) or *CCAR2* knockdown (shCCAR2). $^{**}P < 0.01$, $^{***}P < 0.001$.

RFX1 and CREB have been shown to bind in close proximity to the PCNA promoter (Lee and Mathews, 1997; Liu et al., 1999), suggesting they could contribute to cell cycle control. Given our observations that CCAR2 levels are high in SCC cells compared with keratinocytes (Figure 1b), we examined RFX1 and CREB levels in SCC cells and primary keratinocytes. As with CCAR2, both RFX1 and CREB protein, but not mRNA, were increased in SCC cells (Figure 4b, and see Supplementary Figure S3), suggesting that CCAR2 regulates protein levels of RFX1 and CREB. SIRT1 has been shown to decrease protein stability through deacetylase activity (Li et al., 2010). We hypothesized that CCAR2 inhibits SIRT1-mediated deacetylation through binding to CREB and RFX1, increasing protein stability. Immunoprecipitation of RFX1 from the nuclear and cytoplasmic fractions of HO1N1 cells showed binding of RFX1 to CCAR2 and CREB in the nucleus (see Supplementary Figure S3). Although SIRT1 has been previously found to regulate acetylation of CREB (Paz et al., 2014), RFX1 has not. To determine if RFX1 is also acetylated, we performed immunoprecipitation with α-acetyl lysine antibodies followed by Western blotting for RFX1 in SCC-13 cells, suggesting that RFX1 is acetylated (Figure 4c). Immunoprecipitation with α-SIRT1 antibodies showed that SIRT1 does interact with RFX1 (Figure 4d, and see Supplementary Figure S3). In addition, we also observed binding of CCAR2 to both RFX1 (Figure 4e, and see Supplementary Figure S3) and SIRT1 (see Supplementary Figure S3). CCAR2 controls proliferation, and we sought to examine the interaction of CCAR2 and SIRT1 with RFX1 during the cell cycle. Cells were synchronized before entering S phase with the CDK 4/6 inhibitor PD0332991, released, and then examined during G1 arrest and S-phase entry. Although both CCAR2 and SIRT1 interacted similarly during S-phase entry, there was a shift in the mobility of RFX1 upon S-phase entry. In addition, CCAR2 and SIRT1 appear to physically interact with different forms of RFX1, suggesting that they are in unique complexes (see Supplementary Figure S3). Finally, we sought to examine whether RFX1 and CREB functionally contribute SCC proliferation. Similar to reduction of CCAR2 (Figure 2), shRNA-mediated knockdown of either *RFX1* or *CREB* (see Supplementary Figure S4 online) resulted in a significant increase in G2 phase cells (Figure 5a and b) and a reduction in colony-forming ability (Figures 5c and d). In total, these data support a role for the CCAR2-RFX1-CREB complex in promoting proliferation in SCC tumors.

DISCUSSION

Previous studies have reported conflicting results regarding the role of CCAR2 in tumorigenesis (Chini EN et al., 2013; Song and Surh, 2012), resulting in uncertainty whether CCAR2 would serve as a useful predictive biomarker. Some reports have suggested that CCAR2 is reduced in tumors (Shim et al., 2013; Won et al., 2015), consistent with data from *Ccar2*$^{-/-}$ mice exhibiting an increase in tumor formation (Qin et al., 2015). This also fits with the established role for CCAR2 in regulating stability of p53 through acetylation (Kim et al., 2008; Zhao et al., 2008) or inhibition of the p53 ubiquitin ligase Mdm2 (Qin et al., 2015). Indeed, regulation of p53 by CCAR2 appears to be important for tumor initiation in some tissues, because *Ccar2*$^{-/-}$ mice have increased tumor incidence compared with *wild-type* controls, dependent on p53 but *Sirt* independent (Qin et al., 2015). In contrast to these data, many tumor types have been reported to have high expression of

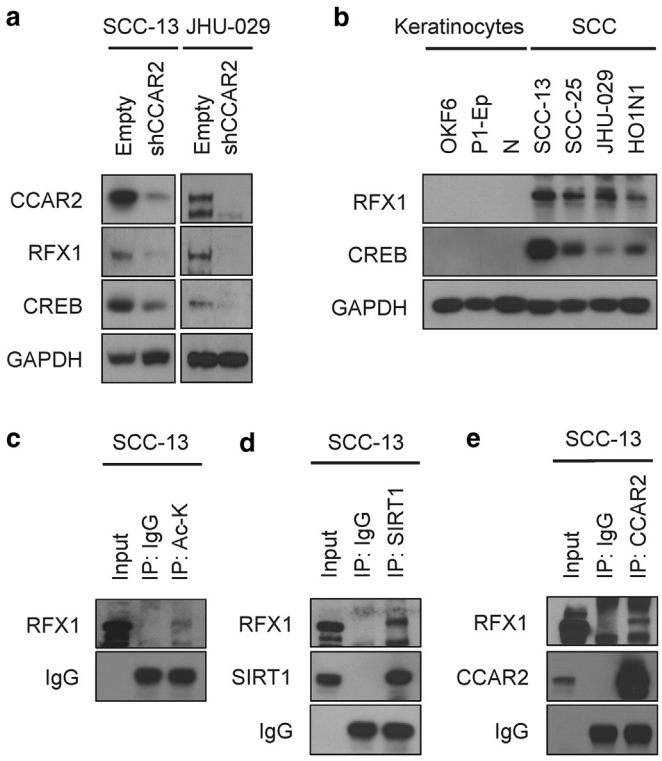

Figure 4. CCAR2 regulates stability of acetylated transcription factors in SCC. (**a**) Western blot analysis of CCAR2, RFX1, and CREB protein in SCC cell lines with *CCAR2* knockdown (shCCAR2) or control (Empty). GAPDH provides the loading control. (**b**) Western blot analysis of RFX1 and CREB protein in keratinocytes and SCC cells. GAPDH provides the loading control. (**c**) Immunoprecipitation of acetylated RFX1 protein from whole-cell extracts of SCC-13 cells. IgG serves as a loading control for IP. (**d**) Co-immunoprecipitation of RFX1 and SIRT1 proteins from whole-cell extracts of SCC-13. IgG serves as a loading control for IP. (**e**) Co-immunoprecipitation of RFX1 and CCAR2 proteins from whole-cell extracts of SCC-13. IgG serves as a loading control for IP. IP, immunoprecipication; SCC, squamous cell carcinoma.

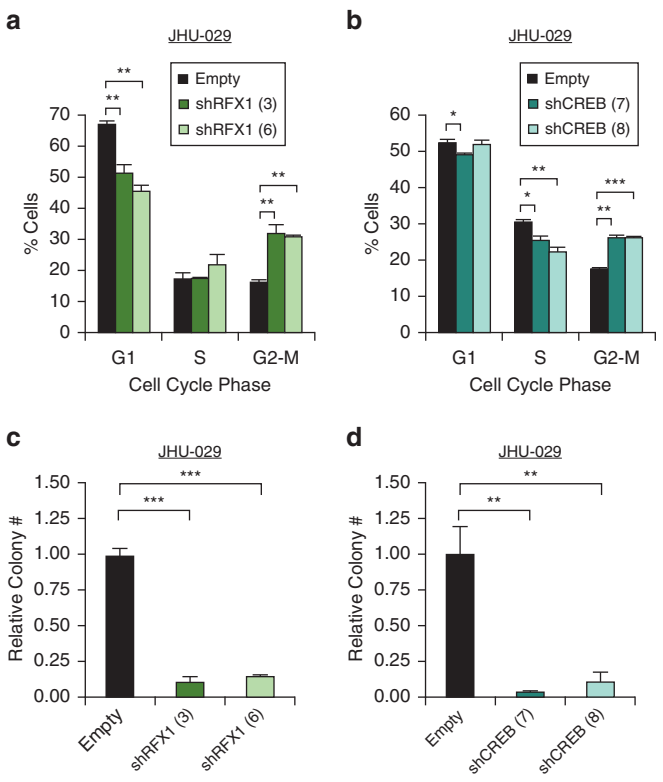

Figure 5. RFX1 and CREB are required for proliferation in SCC. (**a**) Flow cytometry analysis of the cell cycle (G1, S or G2/M) in control (Empty), *RFX1* knockdown (shRFX1), in JHU-029 cells (n = 3). (**b**) Flow cytometry analysis of the cell cycle in control (Empty) or *CREB* knockdown (shCREB) in JHU-029 cells (n = 3). Error bars indicate ± standard deviation. (**c**) Colony assay in control (Empty), *RFX1* knockdown (shRFX1) in JHU-029 cells. Colony number is relative to the control of each cell line. Error bars indicate ± standard deviation. N = 4 replicates per cell line. Representative from two independent repeats. (**d**) Colony assay in control (Empty) *CREB* knockdown (shCREB) in JHU-029 cells. SCC, squamous cell carcinoma. $*P < 0.05$, $**P < 0.01$, $***P < 0.001$.

CCAR2, and this correlates with poor clinical outcomes (Cha et al., 2009; Cho et al., 2015; Kim et al., 2013; Kim et al., 2012; Yu et al., 2016; Yu et al., 2013; Zhang et al., 2014). In addition, the large majority of SCC tumors have mutated or lost *p53* (Giglia-Mari and Sarasin, 2003), whereas *CCAR2* is rarely altered in human cancer (Cerami et al., 2012), suggesting there may be p53-independent roles for CCAR2 in SCC. In this context, we sought to examine the requirement for CCAR2 in established SCC tumors, where high expression of CCAR2 is strongly correlated with poor clinical outcomes (Kim et al., 2012; Yu et al., 2013). Consistent with these reports, we found high levels of CCAR2 in human and mouse SCC compared with normal keratinocytes. This high expression of CCAR2 is functionally important, because reduction of CCAR2 results in decreased proliferation, colony formation, and in vivo tumor growth, strongly supporting a role for CCAR2 in the maintenance of proliferation in *p53*-null tumors. Thus, in addition to serving as a negative prognostic indicator, CCAR2 may serve as an attractive therapeutic target in SCC.

CCAR2 has been shown to affect the activity of a variety of transcription factors in different contexts, serving as a positive regulator of p53 function (Kim et al., 2008; Zhao et al., 2008) but an inhibitor of others such as the liver X receptor-α (Sakurabashi et al., 2015). We have identified an interaction between CCAR2 and the transcription factors RFX1 and CREB, which our data suggest serves to stabilize these proteins. We show a requirement for CREB in maintaining proliferation in SCC cells, and consistent with these data, CREB is required for papilloma formation after chemical carcinogenesis (Rozenberg et al., 2009). Although SIRT1-dependent acetylation of CREB activity has been reported (Paz et al., 2014), CCAR2 was not previously known to be involved in this regulatory axis. To our knowledge, a role for RFX1 in promoting tumor maintenance has not been previously described, and our data show that RFX1 makes a functional contribution to SCC proliferation. Our data also show that RFX1 is an acetylated protein and physically interacts with SIRT1, suggesting that SIRT1 may regulate the RFX1 acetylation state. Regulation of RFX1 stability by SIRT1 fits with a model proposed for the WRN protein, where SIRT1-mediated deacetylation can reduce protein stability (Li et al., 2010). Our data support a model in which CCAR2 functions to maintain appropriate temporal acetylation of RFX1

and CREB by blocking SIRT1 activity and thus facilitating transcription of key cell cycle genes.

MATERIALS AND METHODS

Cell lines and xenografts

The unique identity of SCC-13, SCC-15, SCC-25, JHU-029, and HO1N1 cell lines were verified by short tandem repeat profiling performed by the ATCC. Individual adult B6 mice were used to generate each primary keratinocyte cell line, Mu-K1 and Mu-K2 (see Supplementary Materials online). Culture conditions can be found in the Supplementary Materials. Xenograft tumors were generated as previously described (Ramsey et al., 2011). Four days after injections, water was exchanged with 2% sucrose and 2 mg/ml doxycycline water, or sham water, which was freshly prepared every other day. Tumor volumes were calculated using the formula: tumor volume (mm^3) = $4/3\pi \times (\text{length}/2) \times (\text{width}/2)$.

Western blotting and immunoprecipitation

Cells were lysed in RIPA buffer (10 mmol/L Tris-HCl pH 7.5, 150 mmol/L NaCl, 1 mmol/L EDTA, 1% [weight/volume] sodium deoxycholate, 0.1% [weight/volume] SDS, 1% [volume/volume] NP-40), and Western blotting was performed as previously described (Ramsey et al., 2011). Fractionation of nuclear and cytoplasmic lysates and immunoprecipitation were performed as previously described (Ramsey et al., 2011). In all other immunoprecipitation experiments, cells were incubated at 4 °C for 2 hours with NP-40 lysis buffer (50 mmol/L Tris-HCl pH 7.9, 120 mmol/L NaCl, 0.75% NP-40) and then incubated with protein A beads for 30 minutes. Cleared lysates were incubated with antibody and protein A beads for 3 hours at 4 °C, and immunocomplexes were washed with 5 times with NP-40 buffer. For protein stability experiments, cells were treated with 100 μg/ml cyclohexamide (VWR, Radnor, PA) for up to 8 hours.

Lentiviral infection with shRNA constructs

Lentivirus was generated by transfecting 293T cells using calcium phosphate transfection (Clontech, Mountain View, CA) with plasmid of interest and packaging plasmids (VSV-G, RGR, RSV; Addgene, Cambridge, MA). Viral supernatant was filtered through a 0.45-μm filter, then 8 μg/ml Polybrene (Santa Cruz Biotechnology, Santa Cruz, CA) was added, and viral supernatant was applied to cell lines in six-well plates. After a 1-hour spin infection at 1000*g*, the media was replaced, and puromycin was added to the cells after 24 hours. After 48 hours of incubation with puromycin, cells were harvested for downstream assays. Sequences for hairpins targeting *CCAR2*, *RFX1* (GE Healthcare, Chicago, IL), and *CREB1* (Sigma-Aldrich, St. Louis, MO) are listed in Supplementary Table S6 online.

Cell cycle analysis and colony-forming assays

Cells were treated with 10 mmol/L bromodeoxyuridine (BrdU) 2 hours before trypsinization and fixation with cold ethanol. Cell pellets were incubated in 0.08% (weight/volume) pepsin (in 0.1 mol/L HCl) for 20 minutes at 37 °C and centrifuged. Nuclei were incubated in 2 mol/L HCl for 20 minutes at 37 °C and 0.1 mol/L sodium borate added while vortexing. After centrifugation, pellets were washed in immunofluorescent antibody (IFA) buffer/Tween 20 (10 mmol/L HEPES buffer, 150 mmol/L NaCl, 4% fetal bovine serum, 0.1% sodium azide, 0.5% Tween 20) and incubated in primary BrdU antibody (MoBu-1, Invitrogen, Waltham, MA), washed, and incubated in secondary AlexaFluor488 (Invitrogen). Nuclei were resuspended in IFA with 50 μg/ml propidium iodide for flow cytometry on BD Canto Analyser (BD Biosciences, San Jose, CA) using FlowJo software (FLOWJO, LLC, Ashland OR). For colony-forming assays, 1,000 cells were seeded per well of 12-well tissue culture plates, with media changed every 48 hours. After 8 days, cells were fixed with 10% buffered formalin and stained with 0.1% crystal violet for 20 minutes, and plates were scanned electronically for colony counts. Only colonies meeting a minimum size cutoff were counted.

Quantitative real-time PCR and microarray

RNA was extracted from cell lines using Qiagen (Hilden, Germany) RNeasy Mini Kit according to the manufacturer's instructions. Quantitative real-time PCR analysis was performed using KAPA SYBR FAST ABI Prism qPCR Kit (Kapa Biosystems, Wilmington, MA) according to the manufacturer's instructions. Primers used for quantitative real-time PCR are listed in Supplementary Table S7 online. For microarray analysis, synthesis of cDNA, hybridization, and reading of signal intensity were performed by the Partners HealthCare Center for Personalized Genetic Medicine (Cambridge, MA). RNA quality was assessed on a 2100 bioanalyzer (Agilent, Santa Clara, CA), and total RNA was hybridized to Human HT-12 BeadChip arrays. Chips were scanned with Illumina BeadArray Reader (Illumina, San Diego, CA), and data were processed using the R statistical software environment version 2.12.0 (Gentleman et al., 2004). Data were background corrected, normalized, and underwent variance stabilizing transformation using the Lumi package (Du et al., 2008). Differential gene expression was determined based on a moderated *t* test using the Limma package (Smyth, 2004). Unprocessed raw data are available through the NCBI Gene Expression Omnibus (GSE85966).

Statistical analysis

For cell cycle and colony forming assays, Student *t* test was used to assess statistical significance. For xenograft experiments, *P*-values were determined using multiple-measures analysis of variance. For mRNA correlations, Pearson's product-moment correlation coefficient (R^2) was calculated, and two-tailed *P*-value was generated from a probability table. *P*-values for Gene Ontogeny, Kyoto Encyclopedia of Genes and Genomes (KEGG), and Panther pathways as analyzed using DAVID (National Institutes of Health, Bethesda, MD) were determined using Fisher exact test. Only data sets with a false discovery rate of less than 5% were included. *P*-values less than 0.05 were considered significant for all experiments.

Study approvals

The Partners Human Research Committee approved use of tissues for this study. All human tissue studies used exclusively de-identified and discarded material collected in the course of routine clinical care, for which the Partners Human Research Committee determined that signed informed consent was not required. All animals were housed and treated in accordance with protocols approved by the Harvard Medical Area (HMA) Standing Committee on Animals.

ORCIDs

Matthew Ramsey: http://orcid.org/0000-0003-2402-8502
Sarah Best: http://orcid.org/0000-0002-4232-9432

CONFLICT OF INTEREST

The authors state no conflict of interest.

ACKNOWLEDGMENTS

We wish to thank Rebeca Cardoso, Sandra King, and Pritesh Karia for technical support; James Rheinwald, Chuck Dimitroff, Tobias Schatton, and Norman Sharpless for comments on the manuscript; and James Rheinwald for advice, reagents, and support during the establishment of the Ramsey Laboratory. This work was supported by NCI K99/R00CA157730 (MRR) and the BWH Department of Dermatology Fund for New Investigators.

SUPPLEMENTARY MATERIAL

Supplementary material is linked to the online version of the paper at www.jidonline.org, and at http://dx.doi.org/10.1016/j.jid.2016.09.027.

REFERENCES

Cerami E, Gao J, Dogrusoz U, Gross BE, Sumer SO, Aksoy BA, et al. The cBio cancer genomics portal: an open platform for exploring multidimensional cancer genomics data. Cancer Discov 2012;2:401–4.

Cha EJ, Noh SJ, Kwon KS, Kim CY, Park BH, Park HS, et al. Expression of DBC1 and SIRT1 is associated with poor prognosis of gastric carcinoma. Clin Cancer Res 2009;15:4453–9.

Chen GQ, Tian H, Yue WM, Li L, Li SH, Qi L, et al. SIRT1 expression is associated with lymphangiogenesis, lymphovascular invasion and prognosis in pN0 esophageal squamous cell carcinoma. Cell Biosci 2014;4:48.

Chini CC, Escande C, Nin V, Chini EN. DBC1 (Deleted in Breast Cancer 1) modulates the stability and function of the nuclear receptor Rev-erbalpha. Biochem J 2013;451:453–61.

Chini EN, Chini CC, Nin V, Escande C. Deleted in breast cancer-1 (DBC-1) in the interface between metabolism, aging and cancer. Biosci Rep 2013;33(4).

Cho D, Park H, Park SH, Kim K, Chung M, Moon W, et al. The expression of DBC1/CCAR2 is associated with poor prognosis of ovarian carcinoma. J Ovarian Res 2015;8:2.

Dennis G Jr, Sherman BT, Hosack DA, Yang J, Gao W, Lane HC, et al. DAVID: Database for Annotation, Visualization, and Integrated Discovery. Genome Biol 2003;4:P3.

Du P, Kibbe WA, Lin SM. lumi: a pipeline for processing Illumina microarray. Bioinformatics 2008;24:1547–8.

Escande C, Chini CC, Nin V, Dykhouse KM, Novak CM, Levine J, et al. Deleted in breast cancer-1 regulates SIRT1 activity and contributes to high-fat diet-induced liver steatosis in mice. J Clin Invest 2010;120:545–58.

Gentleman RC, Carey VJ, Bates DM, Bolstad B, Dettling M, Dudoit S, et al. Bioconductor: open software development for computational biology and bioinformatics. Genome Biol 2004;5:R80.

Giglia-Mari G, Sarasin A. TP53 mutations in human skin cancers. Hum Mutat 2003;21:217–28.

Huan Y, Wu D, Zhou D, Sun B, Li G. DBC1 promotes anoikis resistance of gastric cancer cells by regulating NF-kappaB activity. Oncol Rep 2015;34:843–9.

Karia PS, Han J, Schmults CD. Cutaneous squamous cell carcinoma: estimated incidence of disease, nodal metastasis, and deaths from disease in the United States, 2012. J Am Acad Dermatol 2013;68:957–66.

Kim HJ, Kim SH, Yu EJ, Seo WY, Kim JH. A positive role of DBC1 in PEA3-mediated progression of estrogen receptor-negative breast cancer. Oncogene 2015;34:4500–8.

Kim JE, Chen J, Lou Z. DBC1 is a negative regulator of SIRT1. Nature 2008;451:583–6.

Kim JR, Moon YJ, Kwon KS, Bae JS, Wagle S, Yu TK, et al. Expression of SIRT1 and DBC1 is associated with poor prognosis of soft tissue sarcomas. PLoS One 2013;8:e74738.

Kim SH, Kim JH, Yu EJ, Lee KW, Park CK. The overexpression of DBC1 in esophageal squamous cell carcinoma correlates with poor prognosis. Histol Histopathol 2012;27:49–58.

Koyama S, Wada-Hiraike O, Nakagawa S, Tanikawa M, Hiraike H, Miyamoto Y, et al. Repression of estrogen receptor beta function by putative tumor suppressor DBC1. Biochem Biophys Res Commun 2010;392:357–62.

Lee BH, Mathews MB. Transcriptional coactivator cAMP response element binding protein mediates induction of the human proliferating cell nuclear antigen promoter by the adenovirus E1A oncoprotein. Proc Natl Acad Sci USA 1997;94:4481–6.

Li K, Wang R, Lozada E, Fan W, Orren DK, Luo J. Acetylation of WRN protein regulates its stability by inhibiting ubiquitination. PLoS One 2010;5:e10341.

Liu M, Lee BH, Mathews MB. Involvement of RFX1 protein in the regulation of the human proliferating cell nuclear antigen promoter. J Biol Chem 1999;274:15433–9.

Luo J, Nikolaev AY, Imai S, Chen D, Su F, Shiloh A, et al. Negative control of p53 by Sir2alpha promotes cell survival under stress. Cell 2001;107:137–48.

Nin V, Chini CC, Escande C, Capellini V, Chini EN. Deleted in breast cancer 1 (DBC1) protein regulates hepatic gluconeogenesis. J Biol Chem 2014;289:5518–27.

Park SH, Riley PT, Frisch SM. Regulation of anoikis by deleted in breast cancer-1 (DBC1) through NF-kappaB. Apoptosis 2013;18:949–62.

Paz JC, Park S, Phillips N, Matsumura S, Tsai WW, Kasper L, et al. Combinatorial regulation of a signal-dependent activator by phosphorylation and acetylation. Proc Natl Acad Sci USA 2014;111:17116–21.

Qin B, Minter-Dykhouse K, Yu J, Zhang J, Liu T, Zhang H, et al. DBC1 functions as a tumor suppressor by regulating p53 stability. Cell Rep 2015;10:1324–34.

Ramsey MR, He L, Forster N, Ory B, Ellisen LW. Physical association of HDAC1 and HDAC2 with p63 mediates transcriptional repression and tumor maintenance in squamous cell carcinoma. Cancer Res 2011;71:4373–9.

Rozenberg J, Rishi V, Orosz A, Moitra J, Glick A, Vinson C. Inhibition of CREB function in mouse epidermis reduces papilloma formation. Mol Cancer Res 2009;7:654–64.

Sakurabashi A, Wada-Hiraike O, Hirano M, Fu H, Isono W, Fukuda T, et al. CCAR2 negatively regulates nuclear receptor LXRalpha by competing with SIRT1 deacetylase. J Steroid Biochem Mol Biol 2015;149:80–8.

Shim UJ, Lee IS, Kang HW, Kim J, Kim WT, Kim IY, et al. Decreased DBC1 expression is associated with poor prognosis in patients with non-muscle-invasive bladder cancer. Korean J Urol 2013;54:631–7.

Smyth GK. Linear models and empirical Bayes methods for assessing differential expression in microarray experiments. Stat Appl Genet Mol Biol 2004;3:Article3.

Song NY, Surh YJ. Janus-faced role of SIRT1 in tumorigenesis. Ann N Y Acad Sci 2012;1271:10–9.

Tanikawa M, Wada-Hiraike O, Yoshizawa-Sugata N, Shirane A, Hirano M, Hiraike H, et al. Role of multifunctional transcription factor TFII-I and putative tumour suppressor DBC1 in cell cycle and DNA double strand damage repair. Br J Cancer 2013;109:3042–8.

Vaziri H, Dessain SK, Ng Eaton E, Imai SI, Frye RA, Pandita TK, et al. hSIR2(SIRT1) functions as an NAD-dependent p53 deacetylase. Cell 2001;107:149–59.

Won KY, Cho H, Kim GY, Lim SJ, Bae GE, Lim JU, et al. High DBC1 (CCAR2) expression in gallbladder carcinoma is associated with favorable clinicopathological factors. Int J Clin Exp Pathol 2015;8:11440–5.

Yu EJ, Kim SH, Kim HJ, Heo K, Ou CY, Stallcup MR, et al. Positive regulation of beta-catenin-PROX1 signaling axis by DBC1 in colon cancer progression. Oncogene 2016;35:3410–8.

Yu XM, Liu Y, Jin T, Liu J, Wang J, Ma C, et al. The expression of SIRT1 and DBC1 in laryngeal and hypopharyngeal carcinomas. PLoS One 2013;8:e66975.

Yuan J, Luo K, Liu T, Lou Z. Regulation of SIRT1 activity by genotoxic stress. Genes Dev 2012;26:791–6.

Zannini L, Buscemi G, Kim JE, Fontanella E, Delia D. DBC1 phosphorylation by ATM/ATR inhibits SIRT1 deacetylase in response to DNA damage. J Mol Cell Biol 2012;4:294–303.

Zhang Y, Gu Y, Sha S, Kong X, Zhu H, Xu B, et al. DBC1 is over-expressed and associated with poor prognosis in colorectal cancer. Int J Clin Oncol 2014;19:106–12.

Zhao W, Kruse JP, Tang Y, Jung SY, Qin J, Gu W. Negative regulation of the deacetylase SIRT1 by DBC1. Nature 2008;451:587–90.

Zheng H, Yang L, Peng L, Izumi V, Koomen J, Seto E, et al. hMOF acetylation of DBC1/CCAR2 prevents binding and inhibition of SirT1. Mol Cell Biol 2013;33:4960–70.